The observation of the morphology of the fibrous molecular assemblages and the Ni–P microtubes was carried out using a Hitachi S-3000N scanning electron microscope and a Hitachi S-800 field-emission scanning electron microscope. Sample characterizations were performed with a Phillips PW-3050 energy-dispersion X-ray analyzer, a Shimadzu ICP-8100 inductively coupled plasma atomic emission spectrometer, a Shimadzu ESCA 3400 X-ray photoelectron spectrometer, a Bio-Rad FTS6000 Fourier-transform IR spectrometer, and a Rigaku RINT2000 powder X-ray diffractometer.

Received: April 6, 2004
Final version: August 31, 2004

[1] S. E. Frazier, J. A. Bedford, J. Hower, M. E. Kenney, *Inorg. Chem.* **1967**, *6*, 1693.
[2] C. R. Martin, *Science* **1994**, *266*, 1961.
[3] S. Iijima, *Nature* **1991**, *354*, 56.
[4] a) E. J. M. Hamilton, S. E. Dolan, C. M. Mann, H. O. Coloijin, C. A. McDonald, S. G. Shore, *Science* **1993**, *260*, 659. b) P. Gleize, M. C. Schouler, P. Gadelle, M. Caillet, *J. Mater. Sci.* **1994**, *29*, 1575. c) Y. Xia, P. Yang, *Adv. Mater.* **2003**, *15*, 351.
[5] a) J. H. Jung, S. Shinkai, T. Shimizu, *Nano Lett.* **2002**, *2*, 17. b) F. Miyaji, S. A. Davis, J. P. H. Charmant, S. Mann, *Chem. Mater.* **1999**, *11*, 3021.
[6] a) J. Y. Ying, C. P. Mehnert, M. S. Wong, *Angew. Chem. Int. Ed.* **1999**, *38*, 56. b) A. Stein, B. J. Melde, R. C. Schroden, *Adv. Mater.* **2000**, *19*, 1403.
[7] M. Goren, R. B. Lennox, *Nano Lett.* **2001**, *1*, 735.
[8] K. J. C. van Bommel, A. Friggeri, S. Shinkai, *Angew. Chem. Int. Ed.* **2003**, *42*, 980.
[9] a) J. M. Schnur, *Science* **1993**, *262*, 1669. b) B. H. Hong, S. C. Bae, C.-W. Lee, S. Jeong, K. S. Kim, *Science* **2001**, *294*, 348.
[10] S. R. Nicewarner-Pena, G. Freeman, B. D. Reiss, L. He, D. J. Pena, I. D. Walton, R. Cromer, C. D. Keating, M. J. Natan, *Science* **2001**, *294*, 137.
[11] G. Che, B. B. Lakshmi, C. R. Martin, E. R. Fisher, R. S. Ruoff, *Chem. Mater.* **1998**, *10*, 260.
[12] C. J. Brumlik, V. P. Menon, C. R. Martin, *J. Mater. Res.* **1994**, *9*, 1174.
[13] a) J. M. Schnur, *Adv. Mater.* **1994**, *6*, 971. b) W. Shenton, T. Douglas, M. Young, G. Stubbs, S. Mann, *Adv. Mater.* **1999**, *11*, 253.
[14] a) Y. Ono, K. Nakashima, M. Sano, Y. Kanekiyo, K. Inoue, J. Hojo, S. Shinkai, *Chem. Commun.* **1998**, 1477. b) K. Hanabusa, K. Shimura, K. Hirose, M. Kimura, H. Shirai, *Chem. Lett.* **1996**, 885. c) J. H. Jung, K. Yoshida, T. Shimizu, *Langmuir* **2002**, *18*, 8724. d) J. H. Jung, H. Kobayashi, S. Shinkai, K. J. C. van Bommel, T. Shimizu, *Chem. Mater.* **2002**, *14*, 1445.
[15] J. H. Jung, T. Shimizu, *Chem. Lett.* **2002**, 1246.
[16] F. Z. Kong, X. B. Zhang, W. Q. Xiong, F. Liu, W. Z. Huang, Y. L. Sun, J. P. Tu, X. W. Chen, *Surf. Coat. Technol.* **2002**, *155*, 33.
[17] M. Bognitzki, H. Hou, M. Ishaque, T. Frese, M. Hellwig, C. Schwarte, A. Schaper, J. H. Wendorff, A. Greiner, *Adv. Mater* **2000**, *12*, 637.
[18] a) K. Aoki, M. Nakagawa, K. Ichimura, *Chem. Lett.* **1999**, 1205. b) K. Aoki, M. Nakagawa, K. Ichimura, *J. Am. Chem. Soc.* **2000**, *122*, 10997. c) K. Aoki, M. Nakagawa, T. Seki, K. Ichimura, *Bull. Chem. Soc. Jpn.* **2002**, *75*, 2533.
[19] K. G. Keong, W. Sha, S. Malinov, *J. Alloys Compd.* **2002**, *344*, 192.
[20] W. C. Wang, E. T. Kang, K. G. Neoh, *Appl. Surf. Sci.* **2002**, *199*, 52.
[21] X. Q. Zhou, L. W. Li, H. Z. Chena, M. Wang, *Mater. Chem. Phys.* **1999**, *58*, 249.
[22] Y. Zhang, K. L. Tan, G. H. Yang, E. T. Kang, K. G. Neoh, *J. Electrochem. Soc.* **2001**, *148*, C574.
[23] H. Kind, A. M. Bittner, O. Cavalleri, K. Kern, *J. Phys. Chem. B* **1998**, *102*, 7582.
[24] M. Charbonnier, M. Romand, E. Harry, M. Alami, *J. Appl. Electrochem.* **2001**, *31*, 57.

Wax-Protected Catalyst Microspheres for Efficient Self-Healing Materials**

By *Joseph D. Rule*, *Eric N. Brown*, *Nancy R. Sottos*, *Scott R. White*, and *Jeffrey S. Moore**

We have reported a polymeric material that is capable of autonomic crack repair and recovery of structural integrity.[1–5] This self-healing material (Fig. 1a) is a common epoxy which contains solid particles of Grubbs' catalyst and poly(urea-formaldehyde) microcapsules containing liquid dicyclopentadiene (DCPD). When a crack propagates through the epoxy, it also ruptures the microcapsules and releases DCPD into the crack plane. The DCPD then mixes with the Grubbs' catalyst, undergoes ring opening metathesis polymerization (ROMP), and cures to provide structural continuity across the crack plane.

This system performs well with a relatively large (2.5 wt.-%) loading of catalyst, but multiple factors have made lower catalyst loadings ineffective. Firstly, the catalyst does not disperse well in the epoxy, so only a few relatively large (~500 μm) catalyst particles are exposed on the crack plane when low catalyst loadings are used. This poor dispersion of catalyst leads to regions on the crack plane where no catalyst is available to cure the DCPD, and healing is incomplete. Secondly, the epoxy's curing agent, diethylenetriamine (DETA), destructively attacks Grubbs' catalyst as the epoxy initially cures, and this destruction reduces the amount of catalyst that is available for the promotion of healing.[2]

[*] Prof. J. S. Moore, J. D. Rule
Beckman Institute for Advanced Science and Technology
and Department of Chemistry
University of Illinois at Urbana-Champaign
Urbana, IL 61801 (USA)
E-mail: moore@scs.uiuc.edu
Dr. E. N. Brown,[+] Prof. N. R. Sottos
Beckman Institute for Advanced Science and Technology
and Department of Theoretical and Applied Mechanics
University of Illinois at Urbana-Champaign
Urbana, IL 61801 (USA)
Prof. S. R. White
Beckman Institute for Advanced Science and Technology
and Department of Aerospace Engineering
University of Illinois at Urbana-Champaign
Urbana, IL 61801 (USA)
[+] Present address: Material Science and Technology Division, MST-7 and MST-8, Los Alamos National Laboratory, Los Alamos, NM 87545, USA.

[**] The authors gratefully acknowledge support from the AFOSR Aerospace and Materials Science Directorate Mechanics and Materials Program (Award No. F49620-00-1-0094), the National Science Foundation (NSF CMS 0218863), and the Fannie and John Hertz Foundation. Any opinions, findings, and conclusions or recommendations expressed in this publication are those of the authors and do not necessarily reflect the views of the AFOSR. The authors also thank Prof. P. H. Geubelle and Dr. A. J. Jones of the Autonomic Materials Laboratory of the Beckman Institute of Advanced Science and Technology for technical support and helpful discussions.

 DOI: 10.1002/adma.200400607

ADVANCED MATERIALS

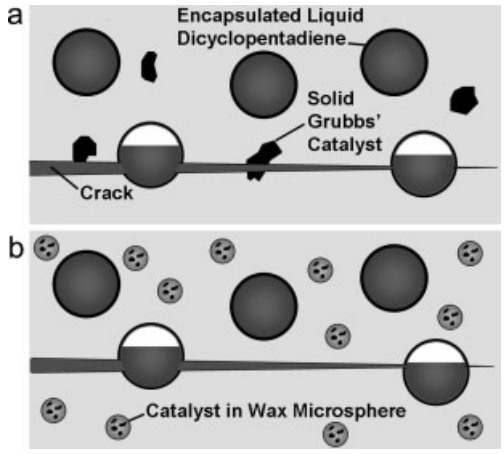

Figure 1. a) Self-healing material using unprotected Grubbs' catalyst. b) Self-healing material with Grubbs' catalyst embedded in wax microspheres.

Taber and Frankowski have shown that Grubbs' catalyst can be incorporated into paraffin wax to protect the catalyst from air.[6] If wax could similarly protect the catalyst from DETA by creating an insoluble barrier between the catalyst and the amine, more efficient use of the catalyst could be achieved. However, for healing to occur when DCPD is released into the crack plane, it must dissolve the wax, release the catalyst, and polymerize to heal the crack.

The wax-protected Grubbs' catalyst was originally reported only as a single monolithic sample,[6] whereas the self-healing application requires small particles that are suitable for distribution in the epoxy. To address this problem, we generated wax microspheres containing Grubbs' catalyst through a hydrophobic congealable disperse phase encapsulation procedure that has been used in similar pharmaceutical applications.[7] These microspheres were synthesized by pouring a mixture of molten wax and bis(tricyclohexylphosphine)benzylidene ruthenium(IV) dichloride (first generation Grubbs' catalyst) into a hot, rapidly stirred, aqueous solution of poly(ethylene-*co*-maleic anhydride).[8] The resulting suspension of molten wax droplets was then rapidly cooled with the addition of cold water to solidify the wax. The wax microspheres were filtered, dried, and sifted to yield a coarse powder. Optical microscopy shows that catalyst particles are suspended in the colorless wax giving the microspheres a speckled appearance, but this heterogeneity is not apparent to the unaided eye.

A model system of wax without Grubbs' catalyst confirmed that the average size of the microspheres can be easily controlled by the rate of stirring. For example, with stirring rates of 450, 900, and 1500 rpm, the average diameters of collected wax microspheres were 150, 90, and 50 μm, respectively. The size distributions are large, but through the use of sieves, narrower size ranges can be isolated. The ethylene–maleic anhydride copolymer is included as a surfactant to facilitate the formation of a suspension. In the absence of copolymer, the average particle size is increased by more than a factor of three, and excessive non-spherical wax debris is formed.

The reactivity of the wax-embedded catalyst was quantified by using in-situ ^{1}H-NMR to measure the ROMP kinetics of endo-DCPD in the presence of the microspheres.[9] The rate constant measured for a sample prepared with the wax microspheres was 2.7×10^{-4} s^{-1}. An analogous control sample prepared with unprotected Grubbs' catalyst had a rate constant of 3.0×10^{-4} s^{-1}, which shows that the process of embedding the catalyst in wax microspheres only reduces the reactivity by 9 %. This small reduction in rate confirms that the catalyst's brief exposure to heat and air only mildly affects its reactivity. Furthermore, when the wax-protected catalyst is melted and cast into new microspheres, the measured rate constant does not change measurably from that of the original microspheres. Because this recycling process can be performed without loss of reactivity, microspheres that fall outside of the desired size range can be reformed with useful diameters, thus avoiding the costly waste of catalyst.

The wax greatly increases the catalyst's resistance to ethylenediamine (EDA). As a control, a sample of unprotected Grubbs' catalyst was exposed to neat EDA and immediately placed under vacuum. Within 10 min, the EDA had completely evaporated. The same procedure was performed with wax-protected catalyst microspheres. NMR samples were prepared using the non-volatile catalyst and wax residues, and the kinetics for ROMP of DCPD were measured for each sample. The wax preserved 69 % of the catalyst's reactivity ($k = 1.9 \times 10^{-4}$ s^{-1}) when the wax microspheres were used, while the unprotected catalyst showed no reactivity. DETA's low volatility prevented it from being used in an analogous experiment, but qualitative tests confirm that it has a similar, minor effect on the catalyst in the microspheres. Therefore, DETA appears to destroy much less catalyst during sample preparation when wax microspheres are used.

The microspheres are also useful for dispersing Grubbs' catalyst uniformly throughout the epoxy matrix. Figure 2a shows a sample of epoxy containing unprotected catalyst (2.5 wt.-%) where typical particles are relatively large and widely spaced. Figure 2b shows a similar sample with microspheres of wax-embedded catalyst (5 wt.-%). Because the wax microspheres contain only 5 wt.-% Grubbs' catalyst, the overall loading of catalyst in the epoxy sample is only 0.25 wt.-%—an order of magnitude lower than the sample in Figure 2a. However, the wax microspheres are well distributed throughout the sample giving a much better dispersion of catalyst particles even with a much lower overall catalyst loading. Thus, the catalyst will be more evenly distributed across the crack plane of a fractured sample. We believe that this more uniform dispersion facilitates healing by providing catalyst to the DCPD on the entire crack plane rather than only to localized areas near isolated catalyst particles.

Using the techniques reported previously,[1,2,4] fracture samples were prepared and tested with 10 wt.-% DCPD microcapsules and various concentrations of catalyst microspheres. Representative virgin and healed load-displacement curves

for a specimen with wax microspheres are shown in Figure 3a. Unlike the behavior reported for self-healing samples prepared with unprotected catalyst (Fig. 3b),[2,4] the self-healing induced with catalyst microspheres exhibits nonlinear elastic behavior. The nonlinearity appears to result from the polyDCPD being plasticized by the wax that is dissolved in the DCPD prior to curing. Separate tensile fracture tests of samples made of polyDCPD with dissolved wax support this explanation (results not shown).

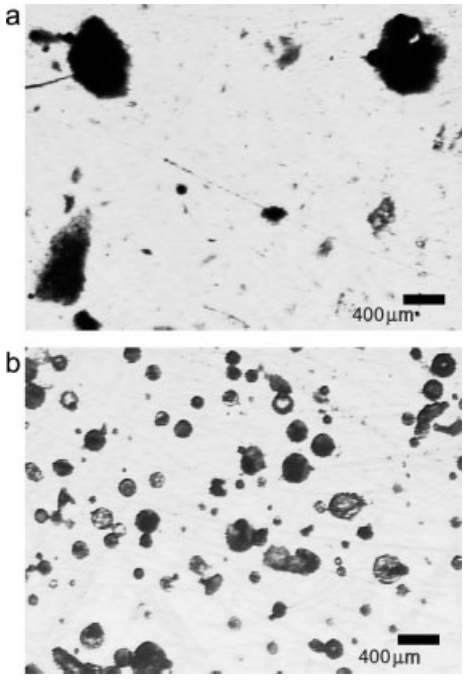

Figure 2. Sections of epoxy samples cut to ~300 μm thick containing a) 2.5 wt.-% unprotected Grubbs' catalyst or b) 5 wt.-% wax microspheres (0.25 wt.-% overall catalyst loading).

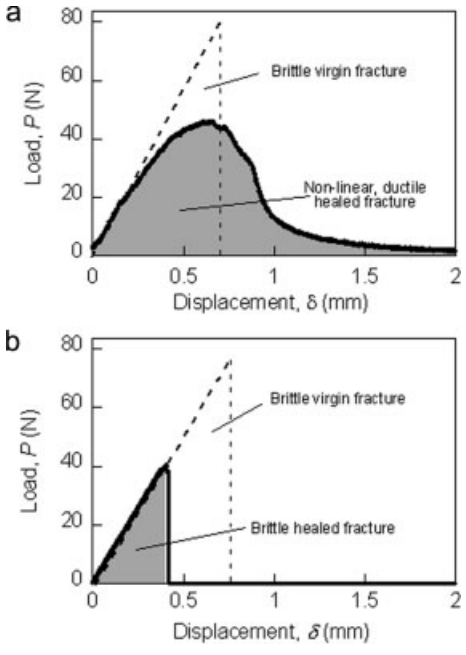

Figure 3. Representative virgin and healed load-displacement curves for samples with a) 5 wt.-% microspheres containing 5 wt.-% Grubbs' catalyst and b) 2.5 wt.-% unprotected Grubbs' catalyst. Both samples contain 10 wt.-% DCPD microcapsules with an average diameter of 180 μm.

Due to the nonlinear response of the healed load displacement curve, the critical fracture toughness (K_{IC}) protocol reported for our previous system cannot be employed.[1,2,4,5] Moreover, while the large-scale initiation of damage and plasticity in the healed interface followed by slow, stable crack growth provides excellent structural recovery and resistance to post-healing failure, a rigorous analysis of fracture properties after healing is beyond the scope of this paper. Thus, the healing efficiency is defined for the current report as the internal work (or strain energy) for the healed sample divided by the internal work for the virgin sample, each normalized by the new surface area generated upon fracture (Eq. 1, see Experimental).

To study the effect that wax has on self-healing, tests were performed with variable amounts of catalyst in the microspheres (Fig. 4a). The loading of microspheres in the epoxy is held constant at 5 wt.-% but the loading of catalyst in the microspheres is varied from 0 % to 25 %. Therefore, the overall amount of catalyst in these epoxy samples ranges from 0 % to 1.25 % (i.e., 5 wt.-% microspheres in epoxy and 25 wt.-% catalyst in microspheres). Not surprisingly, the average healing

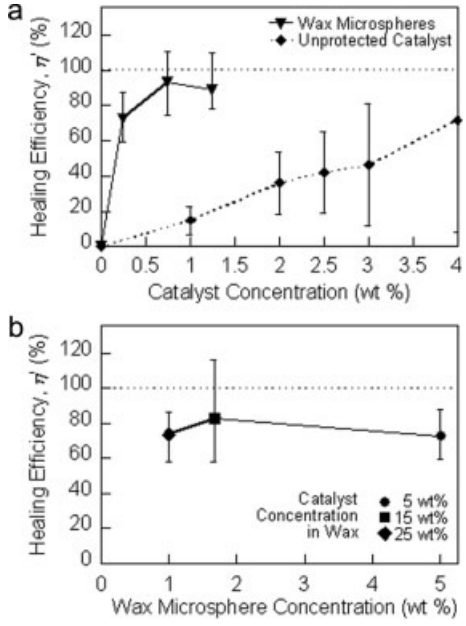

Figure 4. a) Effect of catalyst concentration on healing efficiency for samples with 5 wt.-% wax microspheres and 10 wt.-% DCPD microcapsules or with unprotected catalyst and manually injected DCPD [2]. b) Healing efficiencies achieved with a constant overall catalyst loading of 0.25 wt.-% obtained by simultaneously varying both the amount of catalyst in the wax and the amount of wax in the epoxy. 10 wt.-% DCPD microcapsules were used. The error bars show the total range of results for three trials, and the data points represent the average values.

ADVANCED MATERIALS

efficiency initially increases as catalyst loading increases. However, as the catalyst loading is increased from 0.75 wt.-% to 1.25 wt.-%, the healing efficiency appears to level off, and this may suggest that the maximum average healing efficiency (93 %) can be achieved with just 0.75 wt.-% catalyst loading, a value far below that reported previously for the unprotected catalyst.[1,2,4] When samples with unprotected catalyst were tested using manually injected DCPD to maximize the healing ability, the average healing efficiencies (when recalculated in terms of strain energy release rate) were invariably lower than those achieved with the wax microspheres (Fig. 4a).[2] Moreover, the superior healing efficiencies achieved with the microspheres were possible with catalyst loadings that were about an order of magnitude lower than previously required.

The data in Figure 4a show that a catalyst loading of 0.25 wt.-% is sufficient for very good healing efficiencies. To further investigate this catalyst concentration, a separate series of tests was performed in which the loading of catalyst in the wax was varied inversely with the loading of microspheres in the epoxy in order to maintain a constant overall catalyst level of 0.25 wt.-% (Fig. 4b). Similar healing efficiencies were achieved regardless of the amount of wax in the samples, so healing in this system appears to depend primarily on the overall catalyst loading.

We have shown that Grubbs' catalyst can be embedded into wax microspheres. The samples self-healed with these wax microspheres showed nonlinear elastic fracture behavior with large-scale initiation of damage and plasticity followed by slow, stable crack growth. Even with dramatically reduced catalyst concentrations, the use of microspheres produces healing efficiencies that are superior to those previously achieved. Increased healing efficiency results from more uniform dispersion of the wax-protected catalyst in the epoxy matrix along with the ability of the wax to protect the catalyst from detrimental interaction with DETA. Additional applications of wax-protected catalysts in related self-healing systems are currently being explored.

Experimental

Synthesis of Wax Microspheres Containing Grubbs' Catalyst: In an N_2-filled glovebox, paraffin wax (Aldrich, 10.0 g, mp = 58–62 °C) and Grubbs' Catalyst (Strem, 525 mg) were sealed in a vial. The vial was removed from the glovebox. A solution of water (225 mL), poly(ethylene-*co*-maleic anhydride) (0.63 g, 0.28 wt.-%) and octanol (1 drop) was placed in a 1000 mL beaker in an 82 °C water bath and stirred with a mechanical stirrer at 900 rpm. The vial containing the wax and the catalyst was submerged in the same 82 °C water bath. After 10 min, the wax had melted and the aqueous solution had reached 65–70 °C. The vial with the molten wax was shaken to disperse the catalyst. The vial was then opened (in air), and the wax was poured into the aqueous solution. After 2 min, cold water (600 mL, 0 °C) was quickly added, and the stirring was stopped. The microspheres were collected by filtration and dried under vacuum.

ROMP Kinetics Measurements: In an N_2-filled glovebox, a stock solution of PCy_3 (4.1 mM) in d_8-toluene was prepared. This stock solution was then added to an NMR tube with wax microspheres (140 mg) containing 5 wt.-% Grubbs' catalyst (0.0085 mmol). A control sample with unprotected Grubbs' catalyst (7.0 mg, 0.0085 mmol) and wax microspheres without included catalyst (133 mg) was prepared using the same stock solution of PCy_3 in d_8-toluene. Each solution weighed 0.70 g. The samples were capped with septa and removed from the glovebox. Mesitylene (10 μL) was added via syringe as an internal standard. The ROMP kinetics with *endo*-DCPD were obtained by in-situ ^{1}H-NMR as described previously [9].

Fracture Tests: Fracture samples with a tapered double-cantilever beam (TDCB) geometry were cast from EPON 828 epoxy resin cured with 12 pph DETA containing 10 wt.-% of 180 μm diameter DCPD-filled microcapsules (prepared by in-situ emulsion polymerization) and a prescribed content of wax microspheres [2,4,10]. Samples were cured for 24 h at room temperature followed by 24 h at 30 °C. The samples were pin loaded and tested under displacement control, at 5 μm s^{-1} displacement rate. Samples were tested to failure, the load was then removed, and the crack faces were allowed to come in contact and heal at room temperature. Samples were retested after 24 h.

The protocol established by Brown et al. [1,2,4], to measure crack healing efficiency was modified to account for nonlinearity in the loading trace. Here we define the healing efficiency, η', as the ability to recover internal work (or strain energy) normalized by the new surface area created by fracture:

$$\eta' = \frac{U_{\text{healed}} \Big/ b_n \left(W - a_{0_{\text{healed}}} \right)}{U_{\text{virgin}} \Big/ b_n \left(W - a_{0_{\text{virgin}}} \right)} = \frac{A_{\text{healed}} \Big/ b_n \left(W - a_{0_{\text{healed}}} \right)}{A_{\text{virgin}} \Big/ b_n \left(W - a_{0_{\text{virgin}}} \right)} \quad (1)$$

where U is the internal work (or strain energy) in the sample given by the total area under the load-displacement curve $A = \int_0^{\delta_{\text{failed}}} P(\delta) \mathrm{d}\delta$, b_n is the width of the crack surface created ($b_n = 2.5$ mm), W is the distance from the loading line to the end of the specimen ($W = 79.3$ mm), and a_0 is the initial crack length as determined from initial compliance data. The values for b_n and W are unchanged between the virgin and healed loadings. The initial crack lengths for the virgin tests range from 23–33 mm and depend on the amount of advancement during pre-cracking. The initial crack lengths for the healed samples range from 20–25 mm.

Received: April 22, 2004
Final version: August 2, 2004

[1] S. R. White, N. R. Sottos, P. H. Geubelle, J. S. Moore, M. R. Kessler, S. R. Sriram, E. N. Brown, S. Viswanathan, *Nature* **2001**, *409*, 794.
[2] E. N. Brown, N. R. Sottos, S. R. White, *Exp. Mech.* **2002**, *42*, 372.
[3] M. R. Kessler, S. R. White, *J. Polym. Sci., Part A: Polym. Chem.* **2002**, *40*, 2373.
[4] E. N. Brown, S. R. White, N. R. Sottos, *J. Mater. Sci.* **2004**, *39*, 1703.
[5] M. R. Kessler, N. R. Sottos, S. R. White, *Composites Part A* **2003**, *34*, 743.
[6] D. F. Taber, K. J. Frankowski, *J. Org. Chem.* **2003**, *68*, 6047.
[7] C. M. Adeyeye, J. C. Price, *Pharm. Res.* **1991**, *8*, 1377.
[8] P. Schwab, R. H. Grubbs, J. W. Ziller, *J. Am. Chem. Soc.* **1996**, *118*, 100.
[9] J. D. Rule, J. S. Moore, *Macromolecules* **2002**, *35*, 7878.
[10] E. N. Brown, M. R. Kessler, N. R. Sottos, S. R. White, *J. Microencapsulation* **2003**, *20*, 719.

